

# Al-Fe-Zr (Aluminum-Iron-Zirconium)

V. Raghavan

The previous review of this system by [1992Rag] presented an isothermal section at 900 °C from the work of [1969Bur]. An update by [2003Rag] reviewed a partial isothermal section at 1150 °C determined by [1999Ste]. The update by [2006Rag] reviewed the more complete study of the system by [2004Ste] and presented a liquidus projection, a reaction scheme and two isothermal sections at 1000 and 800 °C. Very recently, two independent thermodynamic descriptions of this ternary system were reported [2008Guo, 2009Rig].

## Binary Systems

The Al-Fe phase diagram [1993Kat] shows that the face-centered cubic (fcc) solid solution based on Fe is restricted by a  $\gamma$  loop. The body-centered cubic (bcc) solid solution  $\alpha$  exists in the disordered  $A2$  form as well as the ordered  $B2$  and  $D0_3$  forms. Apart from the high temperature phase  $\varepsilon$  ( $D_8_2$ ,  $Cu_5Zn_8$ -type cubic; stable between 1232 and 1102 °C), there are three other intermediate phases:  $FeAl_2$ (triclinic),  $Fe_2Al_5$  (orthorhombic), and  $Fe_4Al_{13}$  (monoclinic). The Al-Zr phase diagram [Massalski2] depicts the following intermediate phases:  $ZrAl_3$  ( $D0_{23}$ -type tetragonal),  $ZrAl_2$  ( $C14$ ,  $MgZn_2$ -type hexagonal),  $Zr_2Al_3$  (orthorhombic),  $ZrAl$  ( $B_f$ , CrB-type orthorhombic),  $Zr_5Al_4$  ( $Ga_4Ti_5$ -type hexagonal),  $Zr_4Al_3$  ( $Ir_4Al_3$ -type hexagonal),  $Zr_3Al_2$  (tetragonal),  $Zr_5Al_3$  ( $D8_m$ ,  $W_5Si_3$ -type tetragonal),  $Zr_2Al$  ( $B8_2$ ,  $Ni_2In$ -type hexagonal), and  $Zr_3Al$  ( $L1_2$ ,  $AuCu_3$ -type cubic). The Fe-Zr phase diagram [2002Ste] depicts four intermediate phases:  $Fe_2Zr$  (stable between 1345 and 1240 °C;  $C36$ ,  $MgNi_2$ -type hexagonal),  $Fe_2Zr$  (1673–25 °C;  $C15$ ,  $MgCu_2$ -type cubic),  $FeZr_2$  ( $C16$ ,  $CuAl_2$ -type tetragonal), and  $FeZr_3$  ( $E1_a$ ,  $Re_3B$ -type orthorhombic).

## Ternary Compounds

The ternary phases in this system summarized by [2006Rag] are:  $(Fe,Al)_{12}Zr$  ( $\tau_1$ ) has the  $ThMn_{12}$ -type tetragonal structure.  $FeAl_2Zr_6$  ( $\tau_2$ ) is hexagonal and has a small homogeneity region around the stoichiometric composition.  $Fe_7Al_{67}Zr_{26}$  ( $\tau_3$ ) has the  $AuCu_3$ -type cubic structure. In addition to the above, the  $C14$  and  $C15$  Laves phases occur within the ternary region with a range of homogeneity.

## Ternary Thermodynamic Descriptions

In their thermodynamic description of this ternary system, [2008Guo] used the substitutional solution model

for the liquid, fcc, bcc, and cph phases. The intermetallic phases  $ZrAl_3$ ,  $Zr_2Al_3$ ,  $ZrAl$ ,  $Zr_5Al_4$ ,  $Zr_4Al_3$ ,  $Zr_3Al_2$ ,  $Zr_5Al_3$ ,  $Zr_2Al$ , and  $Zr_3Al$  with limited Fe solubilities were described with two sublattices, with Al and Fe sharing the first sublattice and Zr in the second sublattice. For  $FeZr_2$  and  $FeZr_3$ , two sublattice models of the type  $(Al,Fe,Zr)Zr_2$  and  $(Al,Fe,Zr)(Fe,Zr)_3$ , respectively, were used. The Laves phases  $C14$  and  $C15$  occur not only as binary members ( $Al_2Zr$  and  $Fe_2Zr$ ), but also as phases within the ternary region. An expression of the type  $(Al,Fe,Zr)_2(Fe,Zr)$  was used to describe the Laves phases. The ternary compound  $\tau_1$  was modeled as  $(Al,Fe)_{12}Zr$ . The compound  $\tau_2$  was modeled as  $Fe(Al,Zr)_2Zr_6$ . The third compound  $\tau_3$  was taken to be of a fixed composition. The magnetic contribution to the Gibbs energy was taken into account for the fcc, bcc, and cph phases and for the  $Fe_2Zr$  compound. The binary descriptions of Al-Fe and Al-Zr from the literature were used. The Fe-Zr phase diagram was reassessed by [2008Guo]. Ternary interaction parameters were introduced for the solution phases. The optimized interaction parameters were listed along with those used from literature. The calculated invariant reaction temperatures and compositions were listed and compared with previous work.

In their thermodynamic description, [2009Rig] used the substitutional solution model for the liquid, fcc, bcc, and cph phases. The Fe-based bcc phase was described with a three sublattice model to account for the  $bcc \leftrightarrow B2$  ordering transition. The  $C14$  and  $C15$  Laves phases were modeled as different phases, each with two sublattices. In each sublattice, mixing of all elements (Al, Fe, and Zr) takes place, with Al and Fe mainly present in the first sublattice and Zr on the second. As the two-phase fields between  $C14$  and  $C15$  phases are very narrow [2004Ste], the Gibbs energy surfaces separating them were found to be almost identical by [2009Rig]. The binary phases (other than the Laves phases) were treated by [2009Rig] as stoichiometric compounds with no ternary solubility. The  $\tau_1$  phase was modeled as  $(Al,Fe)_{12}Zr$ , whereas the  $\tau_2$  and  $\tau_3$  were treated as compounds with fixed composition. A ternary interaction parameter was introduced for the liquid phase. The optimized interaction parameters were listed.

The liquidus lines and primary crystallization fields computed by [2008Guo] and [2009Rig] are shown in Fig. 1 and 2, respectively. The details near the Fe-Al side are omitted. Figure 3 shows a superimposition of the two projections. The sections of [2008Guo], which were drawn on isosceles triangles, are suitably scaled to make the comparison. The two projections are generally similar, but some differences. The regions of primary crystallization of  $\tau_2$  do not coincide in the two cases. The fields of primary crystallization of the various Laves phases are also

## Section II: Phase Diagram Evaluations

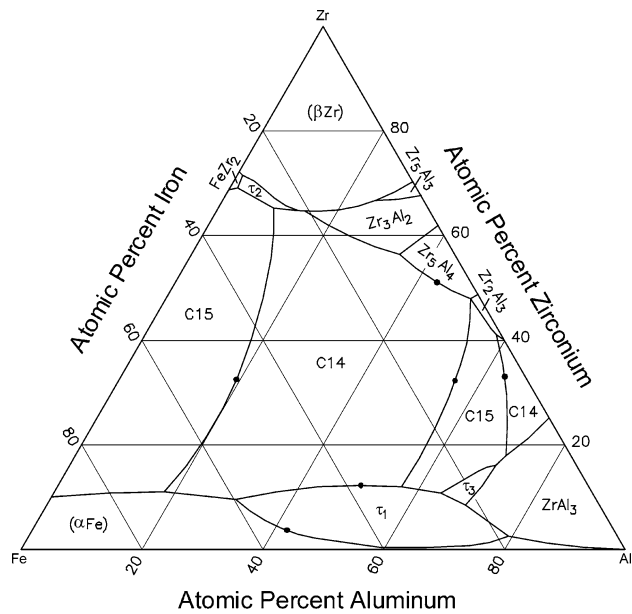


**Fig. 1** Al-Fe-Zr computed liquidus lines and primary crystallization fields [2008Guo]

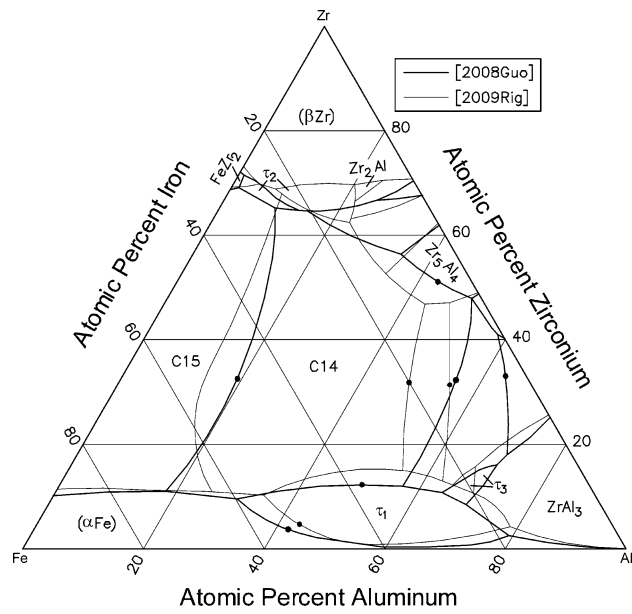


**Fig. 3** Al-Fe-Zr comparison of the computed liquidus lines and primary fields of [2008Guo] and [2009Rig]

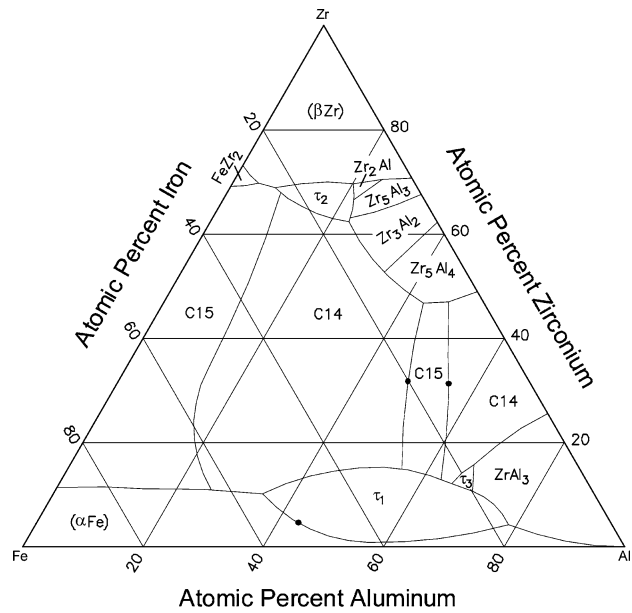


**Fig. 2** Al-Fe-Zr computed liquidus lines and primary crystallization fields [2009Rig]

somewhat different. In Fig. 2, Zr<sub>2</sub>Al nucleates in the ternary region, whereas in Fig. 1 it does not take part in the liquid-solid equilibria.

Figures 4-6 show the computed isothermal section at 1150, 1000, and 800 °C from [2008Guo]. The comparison with the experimental results of [2004Ste] was found to be satisfactory. Figure 7 shows the isothermal section at 900 °C from [2009Rig]. The differences and agreements

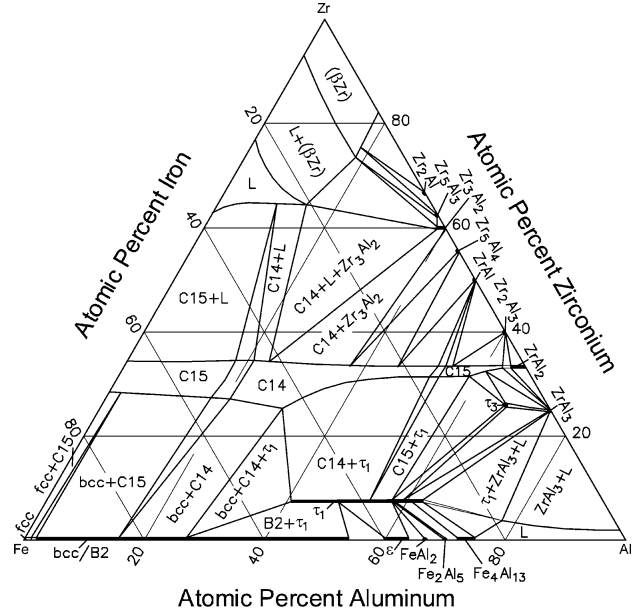


**Fig. 4** Al-Fe-Zr computed isothermal section at 1150 °C [2008Guo]

with the experimental results of [1969Bur] at 900 °C were discussed by [2009Rig].

The width of the two-phase regions separating the Laves phases is in the range of ~1.5-2.5 at.% in the sections computed by [2008Guo], whereas the width is extremely small in the computed sections of [2009Rig]. The width of the two-phase regions between the Laves phases is expected to be not more than 1 at.% [2004Ste], though a precise

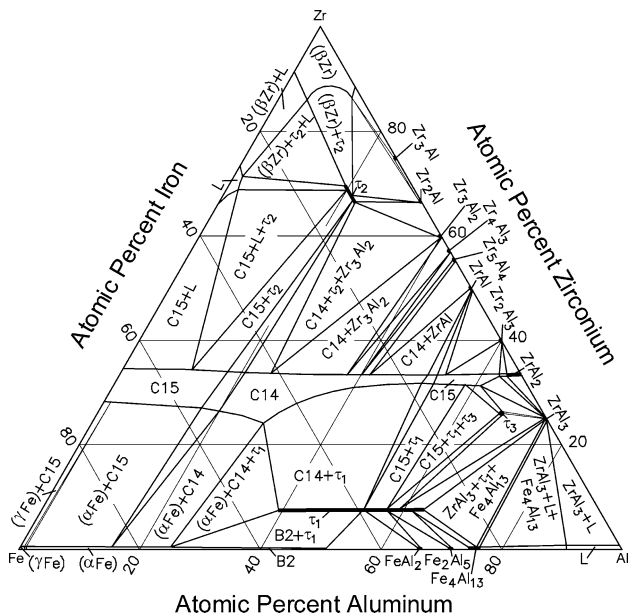


**Fig. 5** Al-Fe-Zr computed isothermal section at 1000 °C [2008Guo]

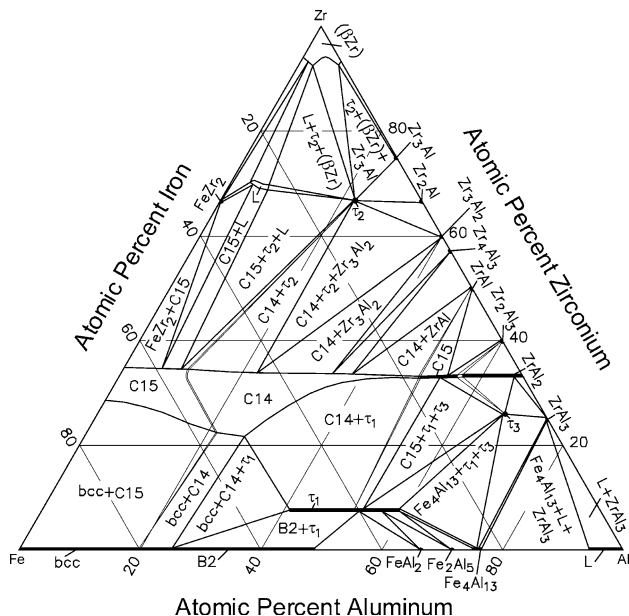


**Fig. 7** Al-Fe-Zr computed isothermal section at 900 °C [2009Rig]

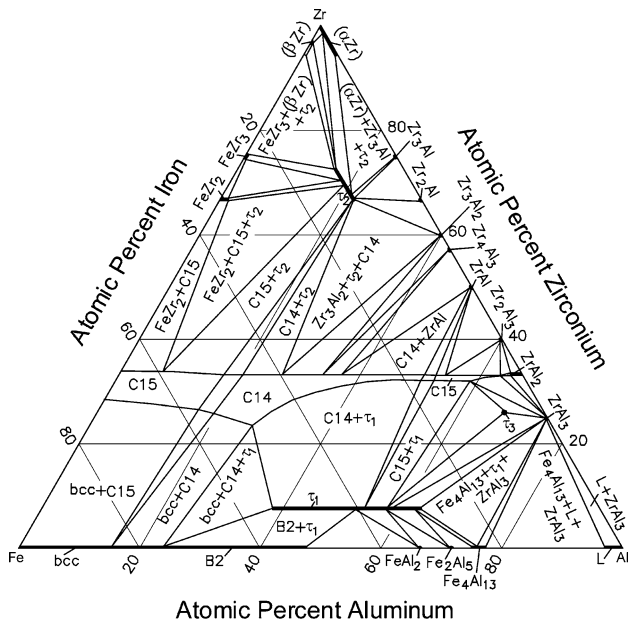


**Fig. 6** Al-Fe-Zr computed isothermal section at 800 °C [2008Guo]. Narrow two-phase regions are omitted

experimental determination is not available at present. In Fig. 8, the Laves phase regions in the two computed results at 1000 °C are superposed.

In conclusion, the differences between the computations of [2008Guo] and [2009Rig] are not much and arise from the different thermodynamic models used and the different emphasis and fit to the experimental data.

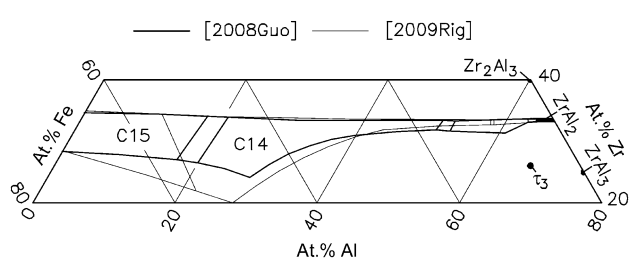


**Fig. 8** Al-Fe-Zr comparison of the Laves phase regions at 1000 °C computed by [2008Guo] and [2009Rig]

## References

- 1969Bur:** V.V. Burnashova and V. Ya. Markiv, Study of the Zr-Fe-Al System, *Dopov. Akad. Nauk Ukr. RSR (A)*, 1969, (4), p 351-353, in Ukrainian

**1992Rag:** V. Raghavan, The Al-Fe-Zr (Aluminum-Iron-Zirconium) System, *Phase Diagrams of Ternary Iron Alloys. Part 6*, Indian Institute of Metals, Calcutta, 1992, p 224-228

**1993Kat:** U.R. Kattner and B.P. Burton, Al-Fe (Aluminum-Iron), *Phase Diagrams of Binary Iron Alloys*, H. Okamoto, Ed., ASM International, Materials Park, p 12-28

**1999Ste:** F. Stein, M. Palm, and G. Sauthoff, Constitution Studies of the Al-Fe-Zr System, *Werkstoffwoche '98, Band VI: Symp. 8, Met. Symp. 14, Simul. Met.*, R. Kopp, Ed., Wiley-VCH Verlag GmbH, Weinheim, Germany, 1999, p 515-520, in German

**2002Ste:** F. Stein, G. Sauthoff, and M. Palm, Experimental Determination of Intermetallic Phases, Phase Equilibria, and Invariant Reaction Temperatures in the Fe-Zr System, *J. Phase Equilib.*, 2002, 23(6), p 480-494

## Section II: Phase Diagram Evaluations

**2003Rag:** V. Raghavan, Al-Fe-Zr (Aluminum-Iron-Zirconium), *J. Phase Equilib.*, 2003, **24**(4), p 350-351

**2004Ste:** F. Stein, G. Sauthoff, and M. Palm, Phases and Phase Equilibria in the Fe-Al-Zr System, *Z. Metallkd.*, 2004, **95**(6), p 469-485

**2006Rag:** V. Raghavan, Al-Fe-Zr (Aluminum-Iron-Zirconium), *J. Phase Equilib. Diffus.*, 2006, **27**(3), p 284-287

**2008Guo:** C. Guo, Z. Du, C. Li, B. Zhang, and M. Tao, Thermodynamic Description of the Al-Fe-Zr System, *CALPHAD*, 2008, **32**, p 637-649

**2009Rig:** V. Rigaud, B. Sundman, D. Daloz, and G. Lesoult, Thermodynamic Assessment of the Fe-Al-Zr Phase Diagram, *CALPHAD*, 2009, **33**, p 442-449